2008

Analysis of Refrigerant Flow Distribution in Evaporators

Junhyeung Kim
Purdue University

James E. Braun
Purdue University

Eckhard A. Groll
Purdue University

Analysis of Refrigerant Flow Distribution in Evaporators

Jun-Hyeung Kim*, Jame E. Braun, and Eckhard A. Groll

Purdue University,
School of Mechanical Engineering,
Ray W. Herrick Laboratories
West Lafayette, IN. 47907, USA

*Corresponding Author: phiengineer@gmail.com

ABSTRACT

Benefits of optimizing refrigerant distribution in evaporators through hybrid-individual superheat control are presented. In order to study the effects of air flow mal-distribution on cooling capacity and COP, a 10.55 kW residential R410A heat pump has been simulated in cooling model. Predictions from the simulation model were then verified through comparisons with measurements. Simulation results show that there are potential benefits in controlling the superheat of individual circuits of evaporators through hybrid-individual superheat control. Two hybrid-individual superheat control methods were studied: upstream refrigerant flow control and downstream refrigerant flow control. Simulation results demonstrate that the upstream refrigerant flow control consistently outperforms the downstream refrigerant flow control, and recovers most of the loss in cooling capacity and COP due to non-uniform air flow distribution.

1. INTRODUCTION

For a given superheat, a vapor compression cooling or heat pump cycle delivers the best system performance when the superheat of each evaporator circuit is uniform. The non-uniform superheat of multi-circuit evaporators can be caused by many factors, including the following: 1) uneven air flow distribution due to air-side fouling, and/or improper design and installation of evaporators; 2) uneven refrigerant flow distribution due to refrigerant-side fouling, and/or manufacturing and design defects of refrigerant distributors; and 3) uneven air-inlet temperature distribution due to air re-circulation. The first and third factors can also induce uneven refrigerant flow distribution in evaporators since the uneven heat flux caused by the air-side flow and/or temperature mal-distributions changes the refrigerant-side flow characteristics.

Many researchers have studied refrigerant mal-distribution in evaporators and its associated impacts on cooling capacity. It has been shown that heat flux and refrigerant flow mal-distributions in evaporators caused by uneven air flow distributions (Domanski 1991) (Payne and Domanski 2003) (Lee et al. 2003), and uneven two-phase flow distributions in distributors (Nakayama et al. 2000) (Li et al. 2005) decrease cooling capacity. In particular, Payne and Domanski (2003) showed that non-uniform superheat at the exit of individual evaporator circuits could decrease cooling capacity even though the overall superheat is maintained. They also demonstrated that much of the decreased cooling capacity could be recovered by individual superheat control.

It appears to be impractical to install conventional superheat controllers on each circuit of the evaporator due to the costs associated with the controllers. Therefore, Braun and Groll (2007) proposed a hybrid-individual superheat control that involves fine-tuning of small valves in each circuit along with using a primary expansion device to control the overall superheat from the evaporator. The primary expansion valve provides most of the necessary pressure drop, whereas the individual valves provide flow balancing of the individual circuits. The flow balancing valves could be located upstream or downstream of the evaporator as shown in Figure 1.

The objectives of this study are to quantify benefits of individual superheat control for a heat pump with specific evaporator and condenser in terms of cooling capacity and system performance and to study the feasibility of using hybrid-individual superheat control.

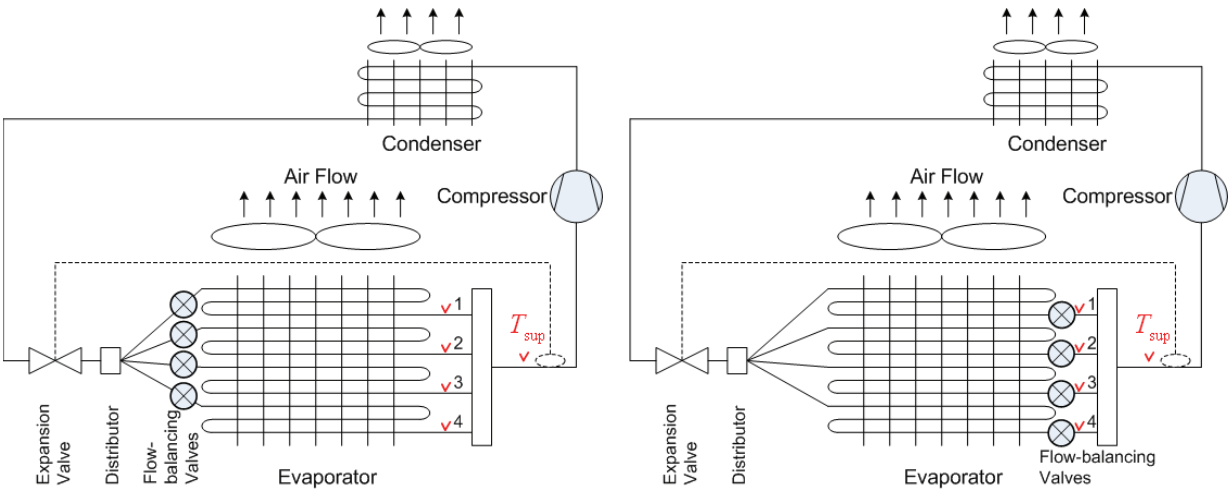

(a) Upstream flow balancing method. (b) Downstream flow balancing method.

Figure 1: Hybrid individual superheat control.

2 SIMULATION OF HYBRID-INDIVIDUAL SUPERHEAT CONTROL

A 10.55kW residential heat pump using R410A was modeled to predict its cooling capacity and system performance in cooling mode. In order to verify the simulation model, the simulation results are compared to measured data. The simulation model was then used to study the effects of air and refrigerant flow mal-distribution on cooling and system performance.

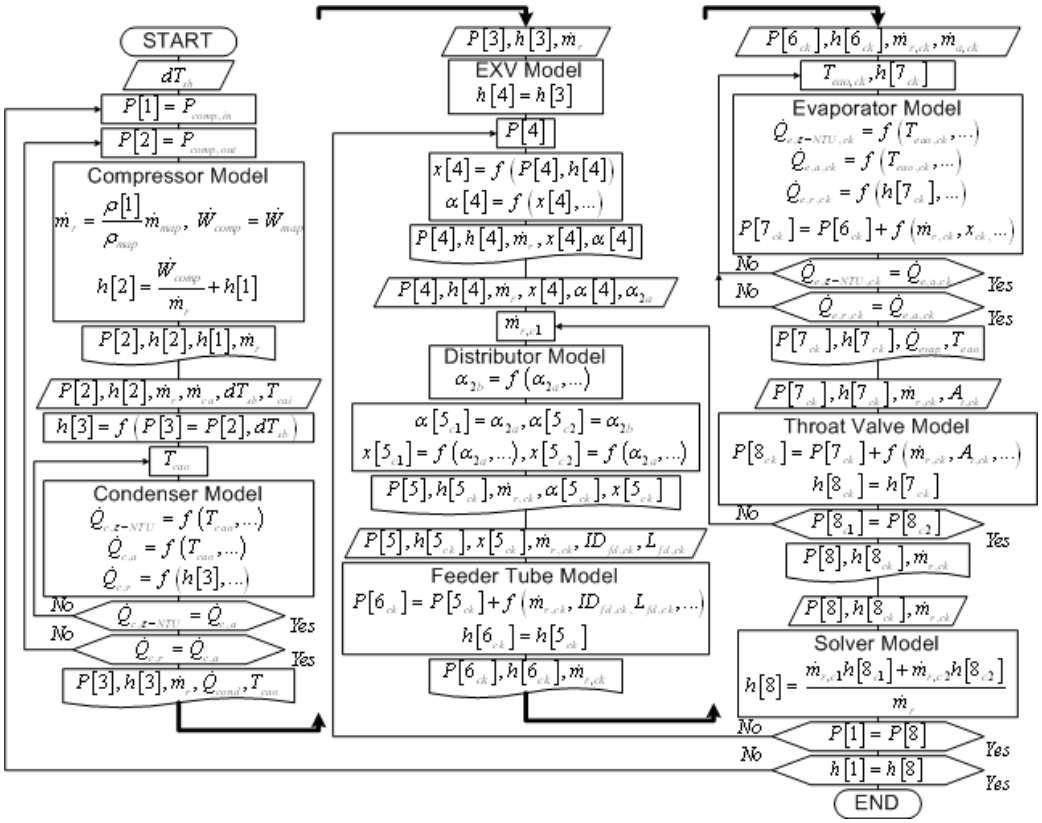

Figure 2: Flow chart of the overall simulation model.

2.1 Description of the simulation model

All components of the heat pump were modeled by writing procedures in Engineering Equation Solver (EES). The simulation model consists of seven sub-models: 1) a map-based compressor model, 2) a lumped condenser model with fixed sub-cooling, 3) an isenthalpic expansion valve model, 4) a distributor model with homogeneous two-phase flow, 5) a feeder tube model, 6) a moving-boundary evaporator model with constant overall superheat, and 7) a throat valve model.

For the purpose of this study, upstream flow balancing was accomplished through adjustments of the diameter of the feeder tubes and downstream adjustments were made by varying the flow area of the throat valve. The pressure drops considered in the model were limited to the primary expansion device, feeder tubes, evaporator, and throat valve. The distributor model did not include frictional losses and was used to determine the exit flow conditions for given inlet conditions. In particular, the distributor model was used to specify mal-distributions in exit refrigerant void fractions under the assumption of homogenous flow. Consideration of pressure drops through the feeder tubes and evaporator allow determination of mal-distributions in refrigerant flow, heat flux, and exit superheat among the different circuits. Under the assumption of constant overall superheat and sub-cooling, the model solves for refrigerant flow distribution of the evaporator, cooling capacity, and efficiency. Figure 2 shows a flow chart of the overall simulation model (a detailed description of the simulation model can be found in Kim et al., 2008).

2.2 Model verification

The simulation results were compared with two sets of measurement data for a 10.55 kW R410A split-system air conditioner using a TXV (Shen et al. 2006): 1) cooling capacity and efficiency data measured at different outdoor temperatures, and 2) cooling capacity and efficiency data measured at different evaporator air flow rates. For each set of comparisons, the simulation results and measurement data were normalized using the largest value of measurement data.

Figure 3 shows a comparison of measured and predicted cooling capacity as a function of outdoor temperature for conditions where the evaporator was not removing moisture. The model predicts cooling capacity with a mean absolute error (MAE) of 1.4 percent and a root mean squared error (RMSE) of 1.6 percent, and captures the downward degradation of cooling capacity as the outdoor temperature increases. Figure 4 shows a comparison between measured and predicted COP as a function of outdoor temperature at dry conditions. The model predicts the COP with a MAE of 4.5 percent and a RMSE of 5.7 percent. It seems that the errors tend to be larger at temperatures below 41.8°C than above. This is mainly because errors in the compressor model predictions of input power consumption are larger at the lower temperatures. Figures 5 and 6 show how well the simulation model predicts cooling capacity and COP at different evaporator air flow rates. The prediction errors tend to increase as evaporator air flow rate decreases. Overall, the model predicts cooling capacity with a MAE of 4.2 percent and a RMSE of 4.6 percent and COP with a MAE of 7.9 percent and a RMSE of 8.0 percent.

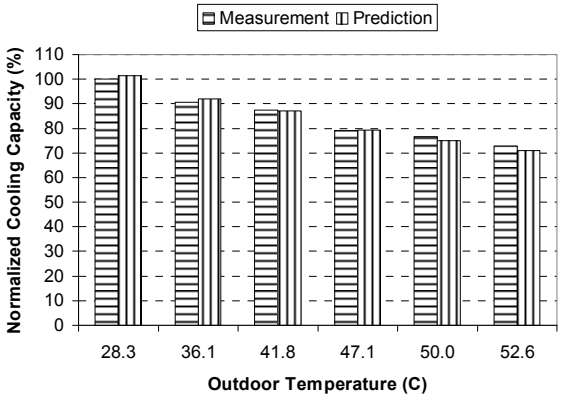

Figure 3: Comparison between measured and predicted cooling capacity as a function of outdoor temperature.

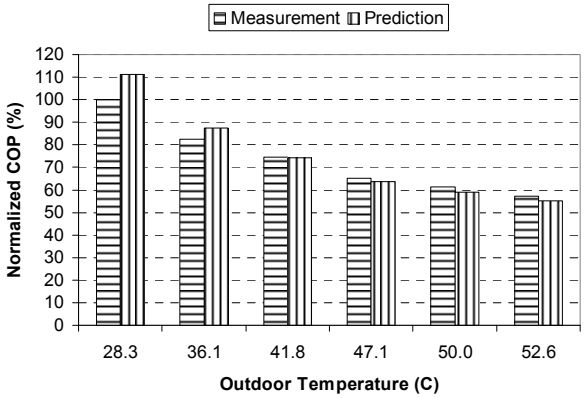

Figure 4: Comparison between measured and predicted COPas a function of outdoor temperature.

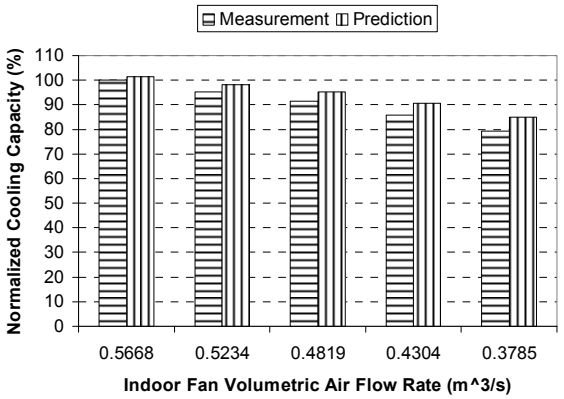

Figure 5: Comparison between measured and predicted cooling capacity as a function of indoor fan volumetric air flow rate.

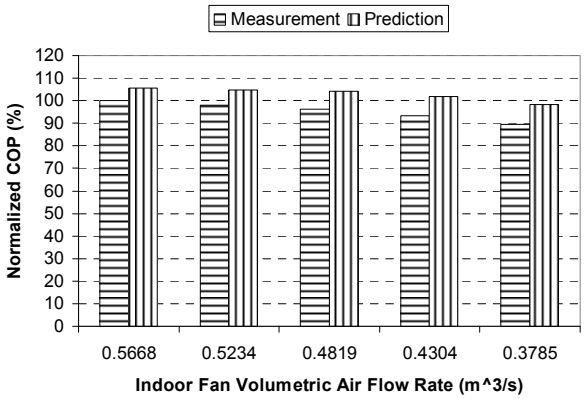

Figure 6: Comparison between measured and predicted COP as a function of indoor fan volumetric air flow rate.

2.3 Analysis of hybrid individual superheat control

Figure 7 presents the configuration of the R410A system model. Each circuit of the evaporator has a feeder tube at the inlet of the circuit and a variable throat valve at the outlet. In practice, upstream or downstream refrigerant flow control would be accomplished using controllable valves. However, for the purposes of this study, the superheat at each outlet of the circuit was controlled by varying either the inside diameter of the feeder tube or the throat area of the variable orifice plate. For instance, when a non-uniform air flows into the evaporator, as depicted in Figure 7, the superheats at the outlets of Circuit 1 (C1) and Circuit 2 (C2) would not be the same. However, by controlling either the inside diameters of the feeder tubes or the throat areas of the variable orifice plates, a uniform exit superheat can be achieved. As a result, some of the reduced cooling capacity due to the non-uniform air flow can be recovered. The current analysis is focused on evaluating the penalty associated with balancing the refrigerant flow downstream of the evaporator (using the variable orifice plate) as compared with upstream refrigerant flow control (using feeder tube adjustments). For all cases, the overall superheat of the refrigerant entering the compressor was the same. Three simulation cases for non-uniform air flow to the evaporator were studied and compared to a base case of uniform air flow:

Case I: system with no refrigerant flow control for individual circuits.
Case II: upstream refrigerant flow balancing control (feeder tube inside diameter control in Figure 7).
Case III: downstream refrigerant flow balancing control (orifice throat area control in Figure 7).

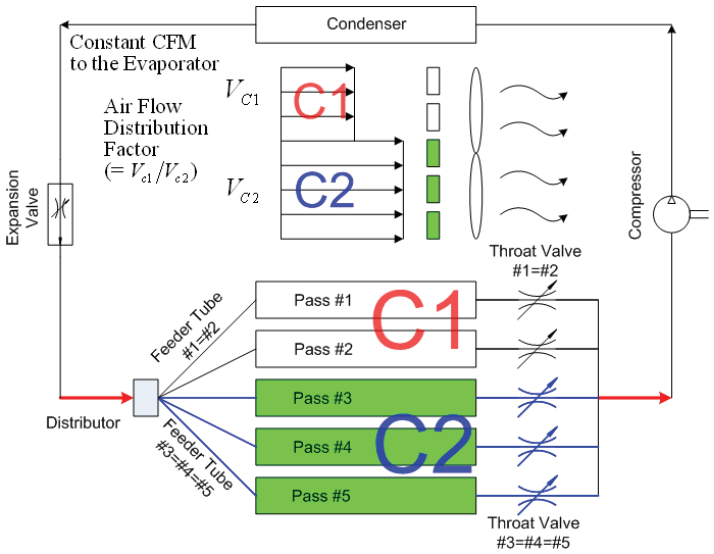

Figure 7: Configuration of the R410A system model.

For each case, the overall volumetric air flow rates of the evaporator and the condenser were kept constant at 0.5663 m^3s^{-1} and 1.347 m^3s^{-1}, respectively. Then, the system was simulated with an overall superheat of 5 K and a sub-cooling of 3 K at dry evaporator coil conditions (an outdoor temperature of 35ºC and an indoor temperature of 26.6°C). In order to simulate air flow mal-distribution, the air flow distribution factor, defined as a ratio of the air flow velocity of Circuit 1 to the air flow velocity of Circuit 2 ($=V_{c1}/V_{c2}$), was introduced. The smaller the air flow distribution factor, the more non-uniform the air flow distribution.

Figures 8 and 9 present that, compared to Case I and III, Case II has insignificant reductions in cooling capacity and coefficient of performance (COP). Compared to Case I, Case III has greater reductions in cooling capacity and COP at the air flow distribution factors of 0.7, 0.8 and 0.9, but smaller degradations at the air flow distribution factor of 0.6. These results demonstrate that upstream refrigerant flow control consistently outperforms downstream refrigerant flow control, and recovers much of the lost cooling capacity and COP due to non-uniform air flow distribution.

Figure 10 shows how the cycle state points in a pressure-enthalpy diagram change at the air flow distribution factor of 0.7 when different individual superheat control methods are applied to the evaporator. It can be seen from Figure 10 (c) that the cycle state points of the upstream refrigerant flow control almost exactly match those of the baseline. This is not the case for the downstream refrigerant flow control. The upstream refrigerant flow control performs much better than the downstream refrigerant flow control because of the large pressure drop at the exit of each pass of Circuit 1 as shown in Figure 10 (d). This large pressure drop can be also interpreted as a throttling loss at the inlet of the compressor.

Figure 11 shows the cycle state points for different air flow distribution factors in a pressure-enthalpy diagram. The superheat of each pass of Circuit 1 decreases as the air flow distribution factor ($=V_{c1}/V_{c2}$) decreases. It is due to the fact that less air flows to Circuit 1, which means that less heat transfer occurs between the air and the refrigerant. On the contrary, the superheat of each pass of Circuit 2 increases because more air flows to Circuit 2 as the air flow distribution factor decreases. It can be also seen from Figure 11 that a decrease in air flow distribution factor causes the evaporating temperature to decrease.

Figure 12 shows that, as the air flow distribution factor decreases (i.e., the non-uniform air flow increases), the total refrigerant mass flow rate decreases. It is also shown that the refrigerant mass flow rates of Circuits 1 and 2 decrease at a similar rate.

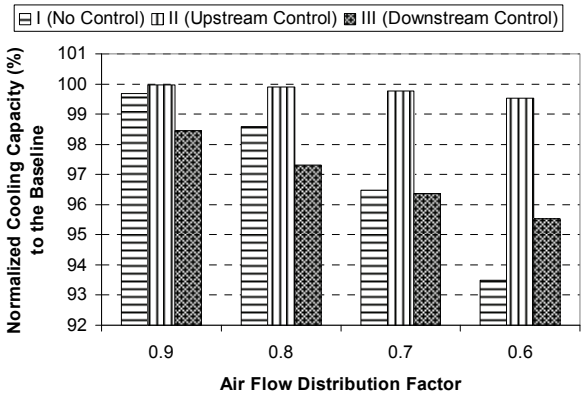

Figure 8: Reduction in cooling capacity compared with uniform air flow as a function of air flow distribution factor.

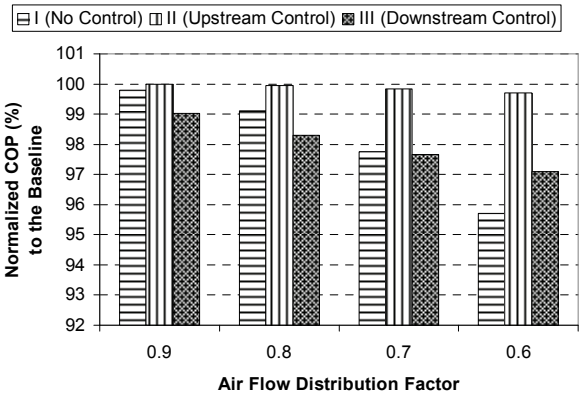

Figure 9: Reduction in COP compared to uniform air flow as a function of air flow distribution factor.

3 SUMMARY

In order to study the feasibility of hybrid-individual superheat control, a 10.55kW residential heat pump using R410A was simulated in cooling mode. The simulation model was verified by comparing simulated results with two sets of actual measurement data: 1) cooling capacity and COP measured at different outdoor temperatures, and 2) cooling capacity and COP measured at different evaporator air flow rates. Both the predicted cooling capacity and COP are in good agreement with the measurements.

The benefits of individual superheat control were then studied using the validated simulation model. A hybrid-individual superheat control method was evaluated that involves fine-tuning of small valves in each circuit along with using a primary expansion device to control the overall superheat from the evaporator. The primary expansion valve provides most of the necessary pressure drop, whereas the individual valves provide flow balancing of the individual circuits. The flow balancing valves could be located upstream or downstream of the evaporator, and both cases were compared with no flow control.

Based on the severity of the air flow mal-distribution, it was found that there could be a significant performance benefit associated with controlling individual refrigerant circuit flow rates using upstream refrigerant flow balancing. However, there is very little benefit in using downstream refrigerant flow balancing control due to the large pressure drop at the exit of the circuit. For a heat pump operating in cooling mode, an air distribution factor of 0.6 was found to reduce cooling capacity by about 6% and COP by about 4%. However, when upstream control of individual circuits was employed to maintain the same superheat at the outlet of each circuit, then more than 99.9% of the loss in cooling capacity and efficiency was recovered.

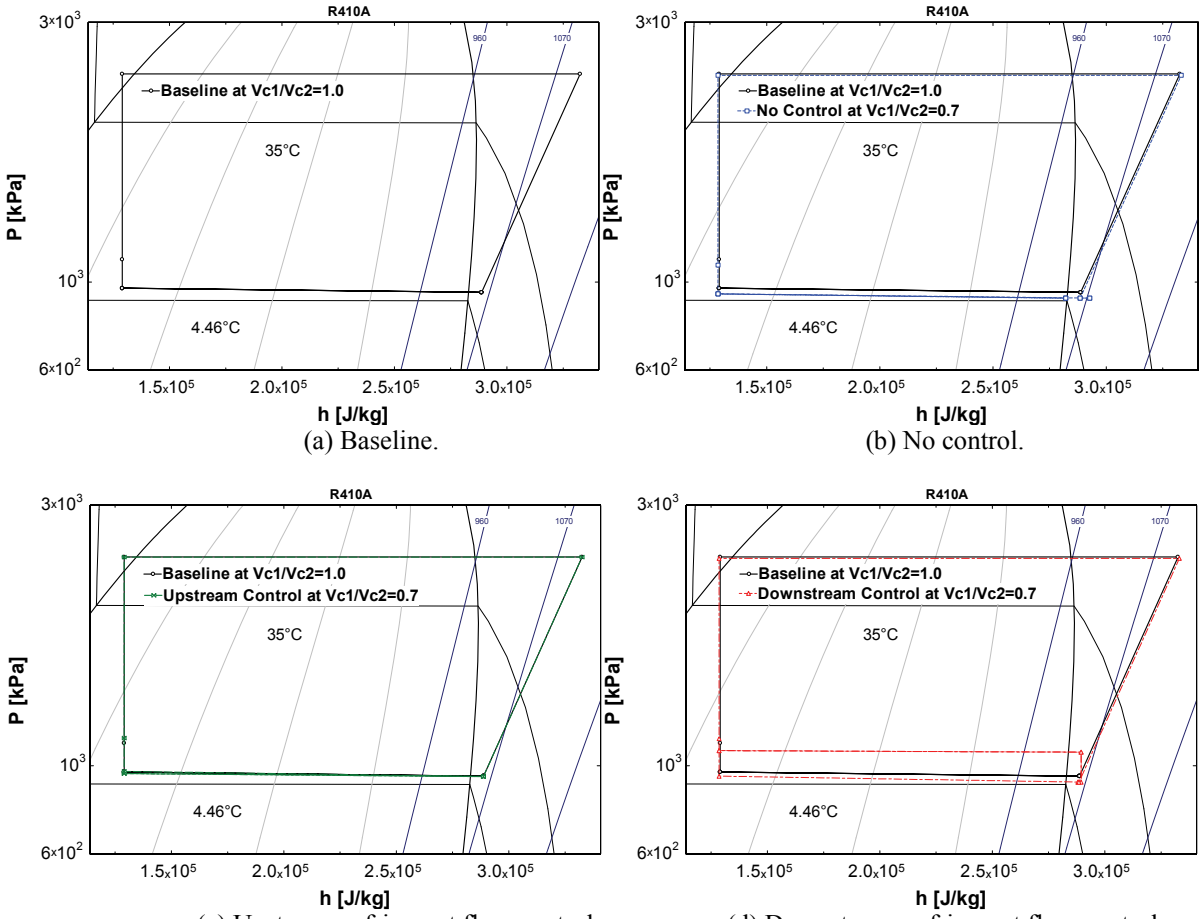

(a) Baseline. (b) No control.

(c) Upstream refrigerant flow control. (d) Downstream refrigerant flow control.

Figure 10: Changes in cycle state points for four different individual superheat controls (a, b, c, and d) in pressure-enthalpy diagrams.

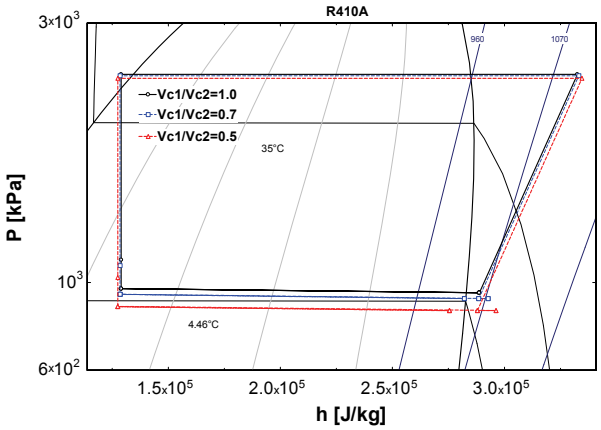

Figure 11: Change in cycle state points as a function of air flow distribution factor for upstream control.

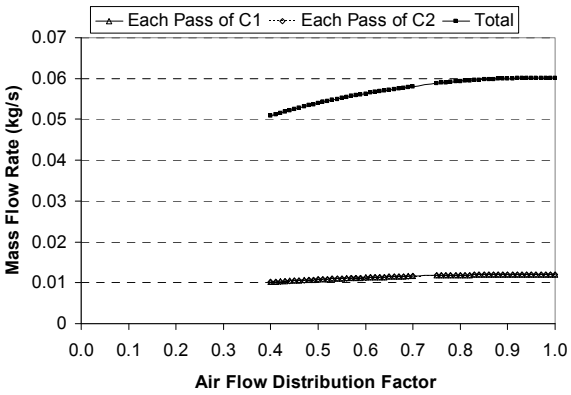

Figure 12: Change in refrigerant mass flow rate as a function of air flow distribution factor for upstream control.

NOMENCLATURE

COP	coefficient of performance
MAE	mean absolute error
RMSE	root mean squared error

V_{c1}	face air velocity at Circuit 1 (m s^{-1})
V_{c2}	face air velocity at Circuit 2 (m s^{-1})

REFERENCES

Braun, J. E., Groll, E. A., 2007, *Proposal for ARTI-06040 project*, Air-Conditioning and Refrigeration Technology Institute, Arlington, VA., USA.

Donanski, P. A., 1991, Simulation of an evaporator with non-uniform one-dimensional air distribution, *ASHRAE Transactions 97,* Issue pt 1, p. 793-802.

EES, *Engineering Equation Solver: Academic Commercial Version 7.938,* F-Chart Software, Madison, Wisconsin.

Kim, J.-H., Braun, J. E., Groll, E. A., 2008, Optimizing refrigerant distribution in evaporators-Phase I, *Final Report No. ARTI-06040,* Air-Conditioning and Refrigeration Technology Institute, Arlington, VA., USA.

Lee, J., Kwon, Y.-C., Kim, M.-H., 2003, An improved method for analyzing a fin and tube evaporator containing a zeotropic mixture refrigerant with air mal-distribution, *International Journal of Refrigeration*, vol. 26, p.707-720.

Li. G., Frankel, S., Braun, J. E., Groll, E. A., 2005, Application of CFD models to two-phase flow in refrigeration distributors, *HVAC&R Research*, Vol. 11, no. 1, p. 45-62.

Nakayama, M., Sumida, Y., Hirakuni, S., Mochizuki, A., 2000, Development of a refrigerant two-phase flow distributor for a room air conditioner, *Proceedings of International Refrigeration Conference at Purdue*, p. 313-319.

Payne, W. V., Domanski, P. A., 2003, Potential benefits of smart refrigerant distributors, *Final Report No. ARTI-21CR/610-20050-01,* Air-Conditioning and Refrigeration Technology Institute, Arlington, VA., USA.

Shen, B., Groll, E. A., Braun, J. E., 2006, Improvement and validation of unitary air conditioner and heat pump simulation models at off-design conditions, *Final Report-1173-RP*, American Society of Heating, Refrigeration, and Air-Conditioning Engineers, Inc.